

## Hierarchical object-based classification of ultra-high-resolution digital mapping camera (DMC) imagery for rangeland mapping and assessment

A.S. Laliberte<sup>a\*</sup>, D.M. Browning<sup>b</sup>, J.E. Herrick<sup>b</sup> and P. Gronemeyer<sup>a</sup>

<sup>a</sup>Jornada Experimental Range, New Mexico State University, PO Box 30003, MSC3JER, NMSU, Las Cruces, NM 88003-8003, USA; <sup>b</sup>USDA Agricultural Research Service, Jornada Experimental Range, PO Box 30003, MSC3JER, NMSU, Las Cruces, NM 88003-8003, USA

Ultra-high-resolution digital aerial imagery has great potential to complement or replace ground measurements of vegetation cover for rangeland monitoring and assessment. This research investigated object-based image analysis (OBIA) techniques for classifying vegetation in southwestern USA arid rangelands with 4 cm resolution digital aerial imagery. We obtained high r-square values for the regressions relating ground- to image-based measures of percent cover (r-square values: 0.82–0.92). OBIA enabled us to automate the classification process and demonstrated potential for quantifying fine-scale land cover attributes with ultra-high-resolution imagery. This approach exhibits promise for nationwide application for monitoring grazing lands.

**Keywords:** aerial photography; object-based image analysis; very high resolution; rangelands; vegetation classification

### 1. Introduction

In the United States, land management agencies such as the Bureau of Land Management (BLM) and the Natural Resources Conservation Service (NRCS) are required to monitor and assess vegetation conditions across millions of acres of grasslands and savannas (i.e. rangelands). Field-based assessments are costly and inefficient over large areas; remote sensing offers the potential to increase the number of monitoring locations, automate the image classification process, and reduce costs of the monitoring. Remote sensing approaches have been tested and implemented for rangeland applications at various spatial resolutions (Weber 2006; Ludwig *et al.* 2007; Laliberte *et al.* 2007; Booth & Cox 2008; Sankey *et al.* 2008). However, the

challenge that remains is developing a remote sensing-based approach that is repeatable, potentially applicable to various vegetation communities, and adapted to imagery of sufficiently high resolution to yield high correlations with ground-based measurements commonly used in national monitoring efforts.

This study is part of a larger research effort focused on developing and testing remote sensing acquisition and analysis techniques for potential integration into the National Resources Inventory (NRI) of grazing lands to enhance assessment of conservation effects. The NRI is a statistical survey of land use and natural resource conditions and trends on U.S. non-federal lands conducted by the National Resources Conservation Service

---

\*Corresponding author. Email: alaliber@nmsu.edu

(NRCS) (Nusser & Goebel 1997). The NRI provides one part of the scientific framework for the Conservation Effects Assessment Project (CEAP), an inter-agency effort to quantify natural resource benefits delivered through conservation actions on private land (Duriancik *et al.* 2008).

As part of NRI, NRCS acquires over 70,000 aerial photos over the USA annually and is in the process of changing from film to digital aerial image acquisition. Currently, only broad land use/land cover classes are determined through photo interpretation. In some cases, such as the 2003 study initiated in southwestern rangelands (Godinez-Alvarez *et al.* 2009), more detailed information is collected through field measurements and observations. However, ground- and image-based measures currently have not been related. There is a keen interest to integrate remote sensing techniques to a greater extent and better correlate ground- and image-derived measurements.

Digital aerial mapping cameras, such as the large format UltraCam, DMC and ADS40 are used to a greater extent than film cameras for aerial photo acquisitions today (Neumann 2008). Compared to film-based products, images acquired with digital mapping cameras have greater radiometric resolution, lower noise levels and are better suited for quantitative remote sensing (Honkavaara & Markelin 2008). The technology has seen increasing use in the last five years, and there is a growing literature of remote sensing applications with digital aerial imagery (Green & Lopez 2007; Coulter & Stow 2008; Rosso *et al.* 2008).

Compared to pixel-based approaches, object-based image analysis (OBIA) with high- or very-high-resolution (<1 m) aerial photography has been shown to yield lower errors and better regression models for urban impervious mapping (Hodgson *et al.* 2003), and higher classification accuracies for detailed vegetation mapping at

the alliance level in California (Yu *et al.* 2006). The ability to segment an image at multiple scales allows for retaining fine-scale vegetation patches within a coarser landscape element (Laliberte *et al.* 2004), and aids in determining appropriate scales for analysis (Laliberte & Rango 2009). Because individual pixels are grouped into homogenous objects, the classification does not suffer from the *salt and pepper* effect of pixel-based classification, and the image objects are ecologically meaningful, whereas individual pixels may not be. The ability to incorporate spatial and contextual features combined with expert knowledge at the object-level allows for greater flexibility in the analysis and improves the classification output (Platt & Rapoza 2008).

In this study, we investigated the use of sub-decimetre resolution (4 cm ground resolved distance) digital aerial imagery for estimating percent cover for vegetation and bare ground using OBIA. The objectives were (1) to compare image-based and ground-based estimates of cover, and (2) to assess the viability and efficiency of applying the image-based method to a broad range of vegetation communities in the region. Future studies will extend these techniques to additional vegetation communities.

## 2. Methods

### *Study area*

Our research was conducted at the Jornada Experimental Range (JER) and the Chihuahuan Desert Rangeland Research Center (CDRRC) in the Jornada Basin of southwestern New Mexico in the northern Chihuahuan Desert (latitude 32°34'11" N, longitude 106°49'44" W) (Figure 1). The area is situated at about 1200 m elevation between the Rio Grande Valley to the west and the San Andres Mountains to the east.

Average monthly maximum temperatures for the JER range from 13°C in

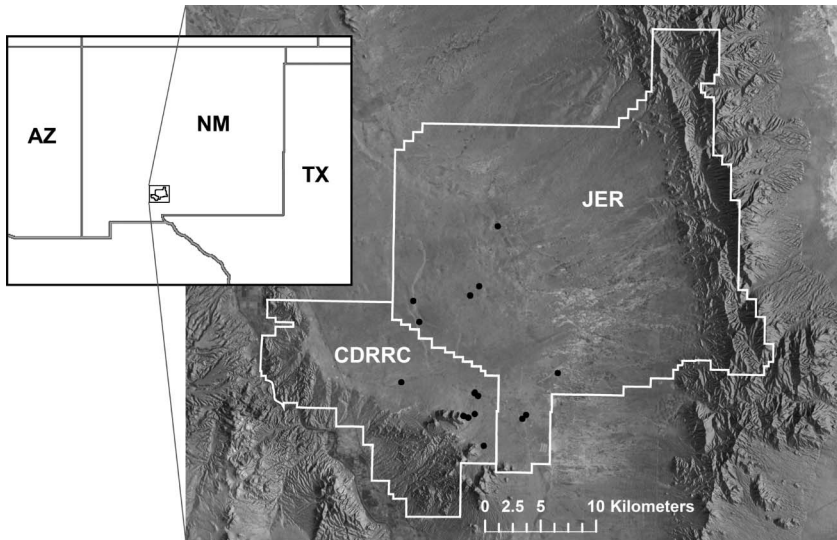


**Figure 1.** Map of study area in southwestern New Mexico at the Jornada Experimental Range (JER) and the Chihuahuan Desert Rangeland Research Center (CDRRC), showing the locations of the 15 sites (black dots), over which the digital aerial imagery was acquired.

January to 36°C in June, and mean annual precipitation is 241 mm, of which more than 50 percent occurs in July, August and September (Wainwright 2006). Rainfall amount and distribution is highly variable. Historically, a large part of the study area was semidesert grassland, but shrub encroachment has led to the conversion to shrubland over the last century (Gibbens *et al.* 2005). Common species include honey mesquite (*Prosopis glandulosa* Torr.), creosotebush (*Larrea tridentata* (Sess. & Moc. ex DC) Cov.), tarbush (*Flourensia cernua* DC.), four-wing saltbush (*Atriplex canescens* (Pursh) Nutt.), soap-tree yucca (*Yucca elata* Engelman.), mormon tea (*Ephedra torreyana* Wats.), broom snakeweed (*Gutierrezia sarothrae* (Pursh) Britt. & Rusby), black grama (*Bouteloua eriopoda* Torrey), tobosa (*Pleuraphis mutica* Buckley), dropseed (*Sporobolus* spp.), threeawn (*Aristida* spp.), and burrograss (*Scleropogon brevifolius* Phil.). Tobosa grasses are more likely to occur in pure stands, while black grama, dropseed and threeawn tend to grow in mixed stands.

The fifteen plots (70 m × 70 m) used in this study were established as long-term research plots as part of the Jornada Basin long-term ecological research (LTER) program. The plots were located in five different vegetation communities (mesquite, tarbush, creosote, grassland, playa) to capture a wide variety of vegetation cover, density, and pattern (Figure 2). The mesquite, tarbush and creosote sites represent shrub-dominated communities, while the grassland and playa sites are grass-dominated.

### Digital imagery

Aerial imagery was acquired over the study plots (one image per plot) on 19 and 21 June 2007 with a large-format digital mapping camera, the Intergraph Z/I Imaging<sup>®</sup> Digital Mapping Camera (DMC). The dynamic range of the DMC imagery is 12 bits, and the image size is 13,824 × 7680 pixels. The multi-head sensor acquires imagery in the red (590–675 nm), green (500–650 nm), blue (400–580 nm) and near infrared (675–950 nm) bands at a coarser

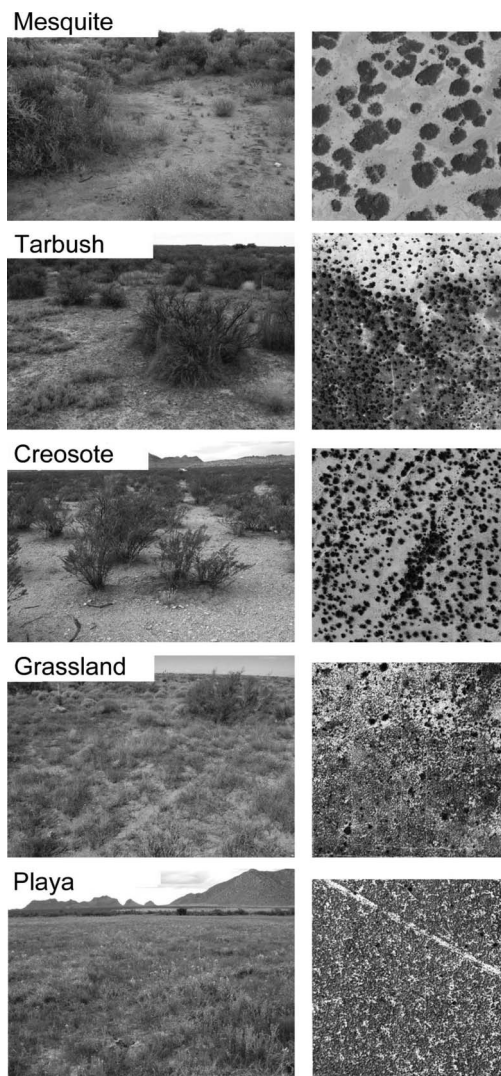


**Figure 2.** Photographs (left column) and digital aerial imagery (right column) of the five vegetation communities assessed in this study. The digital aerial imagery is clipped to the 70 m  $\times$  70 m plots.

resolution, and panchromatic data (400–950 nm) at finer resolution, with a ground sampling distance reduction factor of 4.8. The individual bands are then merged into a pan-sharpened multispectral image (Hinz *et al.* 2000) using a proprietary method. The imagery for this project was acquired at a

flying height of approximately 300 m above ground, which resulted in a ground resolved distance of 4 cm. Imagery was delivered as a three-band colour infrared image (near infrared (NIR), red (R), green (G)).

A subset of each image that encompassed a 90 m  $\times$  90 m area centred on the 70 m  $\times$  70 m plot was georectified to an orthorectified QuickBird image (60 cm resolution). For ground control points, differentially corrected GPS coordinates of the corner fence posts surrounding each plot were used as well as other visible objects, such as large rocks and prominent shrubs. The root mean square error for the polynomial model fit to the GCPs used to calibrate the transformation was < 2 cm.

### Field measurements

Within three weeks of image acquisition, line-point intercept (LPI) data were collected following a standard rangeland monitoring protocol (Herrick *et al.* 2005). LPI data collection was chosen because it is an integral part of the NRI assessment. In each plot, LPI data were collected along four parallel 70 m transects for a total of 280 points/plot (Godinez-Alvarez *et al.* 2009). For each point at a specified distance (i.e., 1 m) along the line transect, a pin is dropped to the ground, and all plant species intercepted by the pin are recorded. In addition, soil surface conditions (e.g., bare, litter, rock) are recorded. Field-based LPI surveys are based on multiple hits per point, but in order to compare results with remotely sensed data, only the top or first intercept of vegetation or soil were used for the analysis. Percent cover by species was derived by dividing the number of hits for each species by the total number of points/plot. Vegetation cover at the species level was aggregated into structure groups (shrubs, grasses, forbs), and then further aggregated into vegetation/non-vegetation

for regression analysis. Species-specific data were used to assess detection limits.

### Digital image analysis

The object-based image analysis program Definiens Developer 7.0.9 (Definiens 2007) was used for image classification. In a first step, an image is segmented into homogeneous areas, and the second step consists of classification of these segments to derive image objects. The segmentation is a bottom-up region merging approach, whereby smaller image objects are merged into larger ones depending on heterogeneity between adjacent image objects. Unit-less parameters (scale, colour and shape) control the segmentation. Colour and shape are weighted from 0 to 1, and within the shape parameter, smoothness and compactness are also weighted from 0 to 1. The scale parameter controls the relative size of the image segments (Baatz & Schaepe 2000; Benz *et al.* 2004).

The images were segmented at 2 levels: (1) a finer multiresolution segmentation (level 1) with scale parameter 50, colour/shape of 0.9/0.1, and smoothness/compactness of 0.5/0.5, and (2) a coarser spectral difference segmentation (level 2) using a maximum spectral difference of 150. The spectral difference segmentation aggregates adjacent image objects with similar spectral responses up to the maximum spectral difference. This allows for combining adjacent image objects with similar spectral properties into larger objects (such as large bare areas) while maintaining small spectrally distinct objects (such as small patches of vegetation) within the bare areas. We used expert judgment and visual interpretation to determine the segmentation parameters. The classifications were performed on the coarser level 2 segmentation.

The objective of this research was to develop a classification approach suitable for multiple images and different vegetation

communities, therefore classes at the top of the hierarchy (left in Figure 3) were common to many sites and generally easier to define, and classes at the bottom of the hierarchy (right in Figure 3) were specific to each site (species-level) and generally more difficult to define. The scheme combined rule-based classification at the top of the hierarchy, and nearest-neighbour classification techniques at the bottom. Shadow/non-shadow, vegetation/non-vegetation, and structure group classes (shrubs, grasses, forbs) were defined with rules and user-defined thresholds.

The suitability of the threshold values that separate two classes in question was assessed with visual interpretation. The *feature view* tool was used, which allowed for visualizing object values for a given feature as a grey-scale image. Classification of litter, bare ground, rocks, grass and shrub species was performed using image-derived samples and nearest-neighbour classification. In sites where litter and/or rocks were

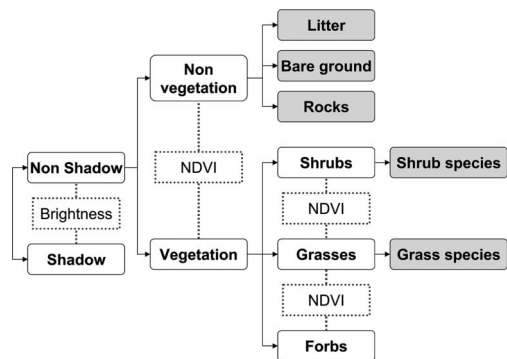


**Figure 3.** The hierarchical classification approach used in the study. Boxes with light background show classes (i.e., land cover types) in bold that were defined using rules with thresholds. Features used for the rules are shown in boxes with dashed outlines (Brightness and Normalized Difference Vegetation Index [NDVI]). Boxes with grey background show classes in bold that were defined using samples and a nearest neighbour classification approach. Please see Table 1 for further description of features.

absent or could not be detected, the non-vegetation class represented bare ground. Likewise, grasses and forbs were grouped if they could not be distinguished separately. The brightness of digital numbers (DN) and the normalized difference vegetation index (NDVI) (Rouse *et al.* 1974) were used as rule-based features. For the nearest-neighbour classification, the means and ratios of the three bands and NDVI were used. The spectral features were used, because they showed the most discrimination for the vegetation of interest. The feature *roundness* was included for sites where broom snakeweed was detected because of the distinctly round growth form of this sub-shrub. The features used in the analysis are described further in Table 1.

In Definiens Developer, the structure and flow control of the entire image analysis procedure (i.e., segmentation, rule-base development, features and samples used, classification) is defined in a process tree. The process tree can be saved and applied to another image, and parameters can be modified easily. This allows for consistency in the analysis and rapid application to multiple images, while still allowing for customization to specific sites. We developed an initial process tree on the first image of a vegetation community and applied it to the next two images in the same vegetation community. The same initial process tree was then applied to the

next vegetation community and so on. This was done to save time and take advantage of similarities in vegetation within a community as well as across different communities, although the process tree required more changes across different vegetation communities compared to within the same community. For each image, the following parameters could be changed, although the same threshold values were used for different images if the results were deemed suitable:

- threshold value for brightness to differentiate shadow and non-shadow
- threshold value for NDVI to differentiate vegetation and non-vegetation
- threshold value for NDVI to differentiate shrubs, grasses, and forbs
- selection of samples for shrub species, grass species, litter, bare ground, and rocks which were unique to each image.

### Statistical analysis

Ground-based LPI measurements and image-derived measurements were expressed as percent cover. For the image analysis product, we summed the pixels for each land cover class and expressed the proportion of each class as percent cover. Regression analysis was used to quantify the relationship between image- and

**Table 1.** Object-based features derived from Definiens Developer and used in the analysis. The column 'Use' describes use of the feature in rule-based (RB) or nearest neighbor classification (NN). Features were calculated for each image object at the level 2 segmentation and are based on digital number (DN) values.

Feature	Use	Description
Mean	NN	Mean of pixels in image object. Computed for NIR, R, and G bands
Ratio	NN	Band mean value of image object divided by sum of all band mean values. Computed for NIR, R, and G bands
Brightness	RB	Sum of mean values of NIR, R, G divided by 3
NDVI	RB/NN	$(\text{Mean NIR} - \text{mean R}) / (\text{mean NIR} + \text{mean R})$
Roundness	NN	Radius of largest enclosing ellipse minus radius of smallest enclosing ellipse

ground-based measurements of percent cover at the structure group level. In addition, paired t-tests ( $n = 15$  plots) were performed to evaluate whether there were statistically distinguishable differences between estimates of land cover from LPI (field) and classified imagery. Species level data were summarized in tabular format.

### 3. Results

#### Segmentation results

Mean object sizes and standard deviations were relatively consistent for the level 1 segmentation (Table 2). The level 2 or spectral difference segmentation showed a greater range in mean object size as well as standard deviation due to the nature of the spectral difference segmentation. Vegetation heterogeneity across sites resulted in retention of smaller, spectrally distinct objects, such as small shrubs, while aggregating larger bare areas.

#### The classification approach

Using the same process tree on multiple images proved to be an efficient approach for classifying vegetation with high-resolution digital aerial imagery. Approximately 8 hours was spent developing the initial process tree. This task involved testing segmentation parameters and determining suitable features for the analysis. On subsequent images, we executed the segmentation and initial classification to the structure group level by using the same thresholds used on the previous image. This initial run was completed in a few seconds. Upon visual inspection, the threshold levels for shadow/non-shadow, vegetation/non-vegetation, and shrubs/grasses/forbs were adjusted. On average, adjusting threshold levels took approximately 20 minutes per image. Further classification to the species level involved selection of samples for each species. Species-specific sample selection

**Table 2.** Number of objects, mean object sizes (in  $m^2$ ) and standard deviations (SD) (in  $m^2$ ) derived from segmentations at two scales for fifteen images of  $70\text{ m} \times 70\text{ m}$  plots. The first letter of each plot denotes the vegetation community (mesquite [M], tarbush [T], creosote [C], grassland [G], playa [P]). The segmentations included a multiresolution segmentation (level 1) with scale parameter 50, colour/shape of 0.9/0.1, and smoothness/compactness of 0.5/0.5, and a spectral difference segmentation (level 2) using a maximum spectral difference of 150.

Plot	Level 1			Level 2		
	No. of objects	Mean object size	Object SD	No. of objects	Mean object size	Object SD
MNORT	79823	0.07	0.07	59842	0.09	0.77
MRABB	97841	0.08	0.09	84412	0.12	0.90
MWELL	72584	0.05	0.07	48106	0.14	1.05
TTAYL	50849	0.08	0.08	24325	0.13	1.11
TEAST	49010	0.07	0.07	33886	0.12	0.95
TWEST	50236	0.06	0.07	32599	0.11	0.88
CCALI	24222	0.08	0.09	20924	0.13	0.78
CGRAV	44543	0.07	0.08	35967	0.12	1.13
CSAND	28117	0.08	0.09	23451	0.12	0.86
PCOLL	78520	0.05	0.07	58456	0.13	0.99
PSMAL	72598	0.05	0.06	53258	0.11	1.04
PTOBO	65230	0.06	0.07	42051	0.13	0.79
GSUMM	33369	0.07	0.07	21436	0.11	0.60
GIBPE	67812	0.08	0.08	44490	0.12	1.30
GBASN	85581	0.07	0.07	66129	0.09	0.39

was most time-consuming, taking from half an hour to an hour depending on vegetation complexity and diversity. The forb class was merged with the grass class, because forbs and grasses were often intermixed and most forbs were too small to be consistently detected in the imagery.

In order to assess the consistency in threshold values from image to image, the range of values (in DN) of a feature (e.g., brightness, NDVI) were plotted and the threshold values (chosen by visual interpretation) used to separate shadow from non-shadow (Figure 4A) and vegetation from non-vegetation (Figure 4B). While the plot-based sample size was small (three plots per vegetation community), it was observed that the threshold values were consistent for each vegetation community. For example, the same brightness threshold value was used to separate shadow from non-shadow for all plots in the creosote-dominated communities (CCALI, CGRAV, CSAND). In addition, communities with no shrubs (all playa sites) had a considerably higher brightness threshold than the shrub-dominated communities.

### Classification to structure group level

The r-square values for image- and ground-based measures of percent cover were relatively high, ranging from 0.823 to 0.924 for the shrub, non-vegetation, total vegetation and grass/forb classes (Figure 5). Paired t-tests indicated statistical differences between the two methods in which the image classification resulted in higher cover estimates for grass/forb (4.5%,  $p = 0.012$ ) and shrubs (2.9%,  $p = 0.038$ ). However, cover estimates for non-vegetation and total vegetation cover were statistically comparable ( $p = 0.302$  and  $p = 0.618$ , respectively). Coefficients of variation were comparable, indicating a similar variability for image- and ground based estimates of cover (Table 3).

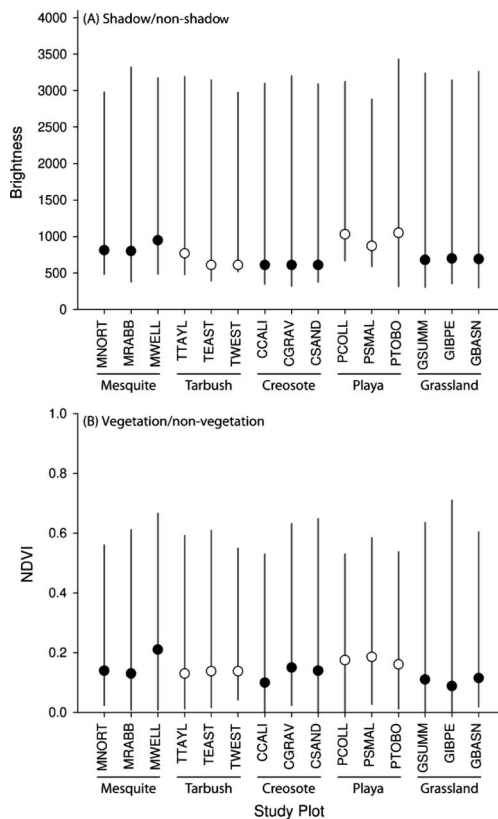


**Figure 4.** Choice of thresholds (black and white dots) in relation to range of DN values (vertical lines) for rule-based classification for the 15 plots. (A) shows the feature brightness used to separate shadow from non-shadow (Shadow/non-shadow). (B) shows the feature NDVI used to separate vegetation from non-vegetation (Vegetation/non-vegetation). All thresholds were chosen by visual interpretation. The three plots in each of the five vegetation communities (identified below the plot names) are grouped together (alternating groups of three black and three white dots). Brightness and NDVI values are derived from digital numbers (DN).

### Classification to species level

Classification to the species level yielded mixed results. We were able to classify dominant shrubs to the species level in every plot where they occurred, but only two prominent grass species, black grama

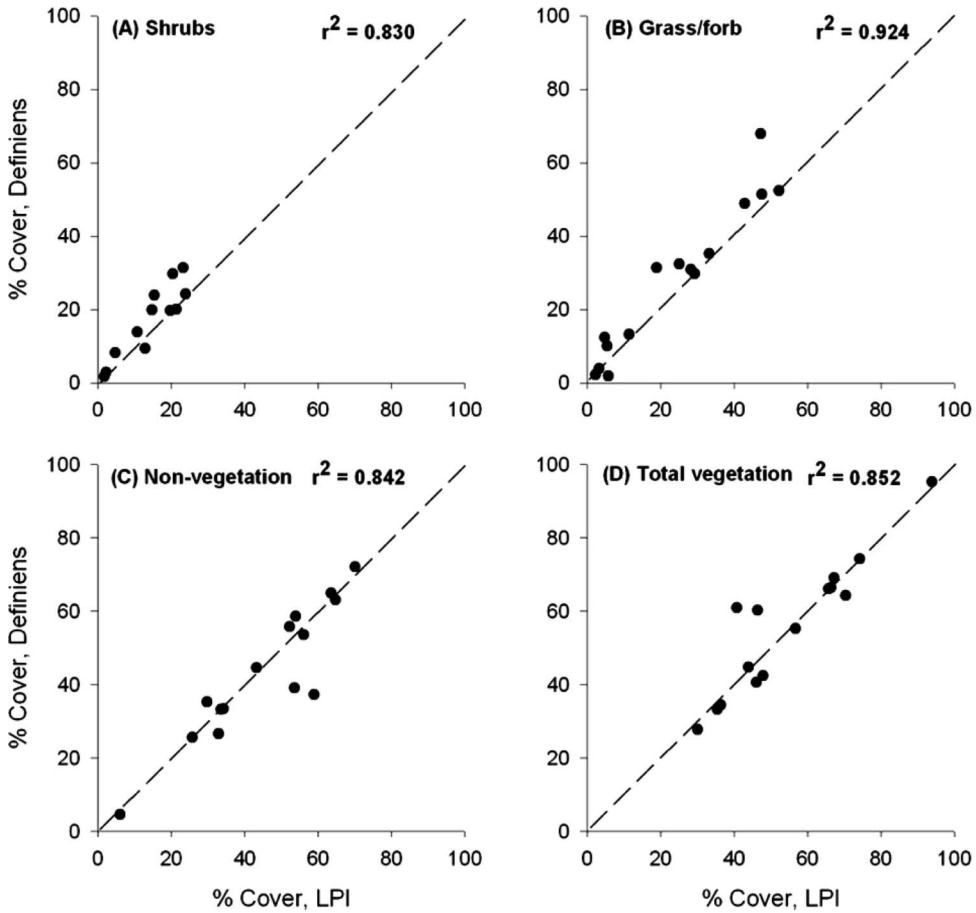


**Figure 5.** Scatter plots for estimates of percent cover obtained with the ground-based line point intercept method (LPI), and from object-based image analysis (DEF) for fifteen 70 m × 70 m plots. Non-vegetation consists of bare ground, rocks and litter. Total vegetation includes litter that is intermixed with vegetation and cannot be detected.

**Table 3.** Results for paired t-tests of differences in percent cover estimates derived from line point intercept (LPI) and image analysis (DEF) methods for 70 m × 70 m plots ( $n=12$  for shrubs,  $n=15$  for all others [three plots had no shrubs]). The mean differences, 95 percent confidence intervals (CI), the means for LPI and DEF, and the coefficients of variation (CV) are shown in percent.

	t-statistic	p-value	Mean diff.	95% CI	Mean		CV	
					DEF	LPI	DEF	LPI
Non-vegetation	-1.07	0.302	-2.0	-5.7-1.7	43.2	45.2	42.0	39.3
Total vegetation	0.51	0.618	0.9	-2.7-4.5	55.7	54.8	32.8	32.4
Grass/forb	2.89	0.012	4.5	1.4-7.5	28.3	23.8	73.1	75.5
Shrubs	2.36	0.038	2.9	0.5-5.2	17.1	14.2	57.9	56.2

Downloaded By: [Laliberte, Andrea] At: 18:44 9 July 2010

and tobosa, were adequately represented in the imagery. Estimates of percent cover from LPI and image analysis for shrub and shrub-like species are compared in Table 4. While there was some variability in the results, the following general observations can be made: (1) shrubs had higher estimates with image analysis, especially large shrubs such as mesquite. With LPI, every gap in the shrub canopy is recorded, while with image analysis, the entire canopy is generally classified as shrub; (2) small

shrubs, such as snakeweed and some saltbush had lower estimates, probably because some of them were missed due to their size (shrubs  $< 12 \text{ cm} \times 12 \text{ cm}$ ); (3) shrub species with percent cover of 1–2 percent based on LPI were generally not detected with image analysis, although there were some exceptions in the grass sites (denoted with *G* as first letter of the plot name in Table 4). The classification of the grassland plot GIBPE is shown in Figure 6. The legend shows the hierarchical classification

**Table 4.** Cover estimates from line point intercept (LPI) and image analysis (DEF) and differences in percent cover between the methods (Diff. = DEF-LPI) for shrubs and shrub-like species for 12 plots (in capital letters). The first letter of each plot denotes the vegetation community (mesquite [M], tarbush [T], creosote [C], grassland [G]).

	LPI	DEF	Diff.		LPI	DEF	Diff.
<b>MNORT</b>				<b>TTAYL</b>			
Shrubs total	23.20	31.41	+8.21	Shrubs total	14.64	19.89	+5.25
Mesquite	18.57	26.60	+8.03	Tarbush	14.28	19.89	+5.61
Saltbush	4.27	3.97	-0.30	Wolfberry	0.36		
Snakeweed	0.36	0.85	+0.49				
<b>MWELL</b>				<b>TEAST</b>			
Shrubs total	21.43	23.82	+2.39	Shrubs total	10.71	13.94	+3.23
Mesquite	15.00	21.65	+6.65	Tarbush	9.28	13.94	+4.66
Snakeweed	5.71	0.85	-4.86	Wolfberry	1.07		
Saltbush	0.36	1.32	+0.96	Mesquite	0.36		
Ephedra	0.36						
<b>MRABB</b>				<b>TWEST</b>			
Shrubs total	20.36	27.23	+6.87	Shrubs total	12.86	9.34	-3.52
Mesquite	11.79	22.96	+11.17	Tarbush	12.50	9.34	-3.16
Saltbush	5.00	2.51	-2.49	Wolfberry	0.36		
Snakeweed	3.57	1.76	-1.81				
<b>CSAND</b>				<b>GBASN</b>			
Shrubs total	23.93	24.29	+0.36	Shrubs total	3.21	2.58	-0.63
Creosote	21.43	24.29	+2.86	Mesquite	1.07	1.27	+0.20
Mesquite	2.14			Snakeweed	1.07	0.94	-0.13
Ephedra	0.36			Yucca	1.07	0.37	-0.70
<b>CGRAV</b>				<b>GIBPE</b>			
Shrubs total	19.64	19.75	+0.11	Shrubs total	9.29	8.29	-1.00
Creosote	16.07	17.87	+1.80	Mesquite	3.57	4.94	+1.37
Mesquite	1.79	1.88	+0.09	Snakeweed	4.29	2.59	-1.70
Sumac		1.07		Yucca	0.36	0.76	+0.40
Tarbush	0.71			Ephedra	1.07		
<b>CCALI</b>				<b>GSUMM</b>			
Shrubs total	21.43	20.11	-1.32	Shrubs total	2.14	2.82	+0.68
Creosote	21.43	20.11	-1.32	Creosote	1.42	2.16	+0.74
				Yucca	0.36	0.66	+0.30
				Ephedra	0.36		

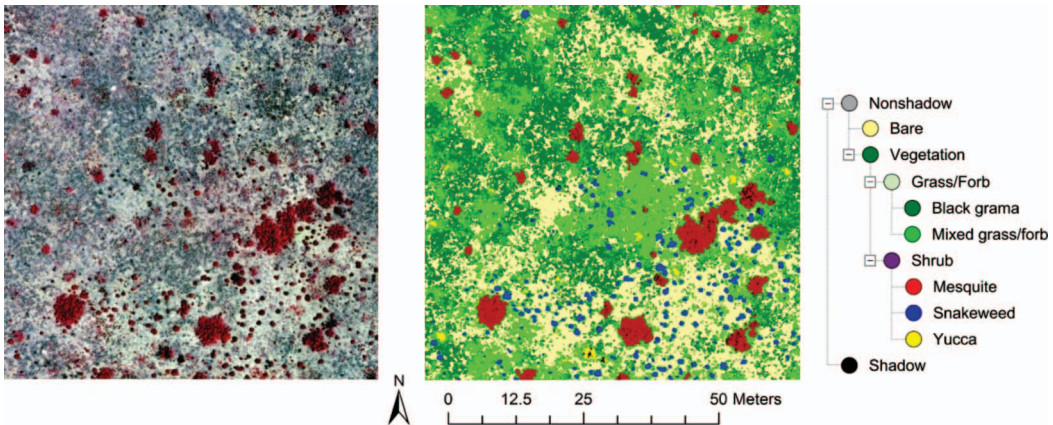


**Figure 6.** DMC colour-infrared image (left) and classification (right) of the grassland plot GIBPE.

approach, which allows for collapsing the classes to the structure group level or to the bare/vegetation level.

#### 4. Discussion and conclusions

In this study, we compared image and ground-based measures of percent cover and assessed the viability and efficiency of applying the image-based method to sites with a wide range in vegetation composition and structure. The OBIA approach performed well using sub-decimetre resolution imagery. Generalizing groups of pixels into segments is nearly essential for meaningful classification of this imagery due to the high degree of spectral variability within a single shrub canopy or patch of vegetation. High correlations were obtained with ground-based measurements for total vegetation, shrubs, grasses and non-vegetated surfaces. At the species level, grasses were difficult to delineate and large shrub species exhibited the greatest disparity between estimated cover for field- and image-based methods. Image estimates were consistently higher than LPI field estimates presumably due to differences in field perception of gap fraction and nadir depictions of vegetation on which the image analysis was based.

While the radiometric and spatial resolution of the DMC digital imagery was high, difficulties were still encountered in mapping certain species. Grasses were especially difficult to separate by species for several reasons. First, grass species such as dropseed and threeawn are bunchgrasses and individual plants or patches are difficult to identify due to their small size. Second, many grass species grow in mixed stands which are not spectrally distinct. Third, in this semi-arid environment, many patches contain both senescent and photosynthetic (i.e., green) components of the same species. Because we did not have spatially explicit training sites to delineate patches by species, we had to rely on information that could be extracted visually from the imagery; only black grama and tobosa grasses exhibited unique spectral and textural properties that permitted identification by species.

Due to the relatively recent introduction of digital aerial mapping cameras, very few studies are available for comparison, and those available tend to employ coarser resolution imagery. Rosso *et al.* (2008) compared four digital airborne sensors for land surface mapping with imagery ranging from 10 to 40 cm spatial resolution, but

their objective was to evaluate and compare the performance of the sensors for land cover mapping, not to evaluate transferability of non-traditional image classification algorithms. Stow *et al.* (2008) quantified change in a 1 km<sup>2</sup> shrubland habitat preserve in southern California over 8 years using 1 m resolution digital aerial imagery. Our objective was to develop and evaluate a semi-automated image classification protocol with sub-decimetre resolution digital imagery to permit analysis of multiple sites across a range of land cover conditions.

This research determined that the application of a well-developed process tree iteratively to subsequent images had several advantages. Those included faster processing of multiple images, ease of comparison of results from different sites, and the ability to expand or collapse the hierarchical classification scheme for management decisions at different levels of detail (i.e. vegetation/non-vegetation, structure group or species level). For example, an estimate of the amount of non-vegetation at the plot level is related to bare ground, which is an important indicator of rangeland health because of the potential for wind and water erosion in areas of exposed soil (Pellant *et al.* 2005).

A potential disadvantage of transferring an image analysis approach to multiple images is that the procedure may not perform consistently across all vegetation communities. For example, the separation of vegetation and non-vegetation using NDVI may not be suitable if the proportion of senescent vegetation is high. A different segmentation scale may also be necessary for certain sites. Because all vegetation communities in this study were located in the Chihuahuan desert consisting of different arrangements of similar species with comparable spectral properties, the segmentation and workflow parameters were broad enough to apply to all images. With this

high-resolution imagery, the appropriate segmentation scale was relatively easy to identify visually. If this technique was applied to sites in other eco-regions, we anticipate that different process trees for each of these sites would probably have to be implemented.

A prime motivation for this study was to develop an approach for the NRI for image-based assessments of plots over spatially extensive and often remote areas that may not be visited in the field. Therefore, we had to rely on visual interpretation of structure groups/species in the plot. While the species list from LPI was available to us for image analysis, LPI data are not designed for validating remotely sensed imagery but represent a repeatable method to quantify changes in land cover conditions. Derivation of image sample objects for object-based classification is not possible using LPI data that correspond to a different scale of observation. LPI data represent very fine-scale measurements; LPI measurements are derived by dropping a pin at specified intervals along a line transect to record multiple levels of vegetation and surface components that the pin hits. If the pin hits a single blade of grass over a bare patch, it is recorded as grass. In OBIA, the same location would in all likelihood be classified as a bare patch. This discrepancy highlights existing challenges relating LPI information to remotely sensed imagery.

We believe additional ground measurements are needed and suggest the collection of spatially explicit training samples, consisting of polygons depicting specific species or vegetation patches. These polygons are more suitable to OBIA than point-level field measurements (Laliberte *et al.* 2007). The issue of identifying appropriate image samples is confounded by the challenge of co-registering spatially explicit field data to sub-decimetre imagery with sufficient location accuracy. Even

differentially corrected GPS data have sub-metre levels of error, which is relatively large when those data are overlaid on 4 cm resolution imagery. However, given the assumed errors, it is easier to determine whether a polygon is *off* with regard to the image than determining the location of a point. It is planned to incorporate GPS-based training samples in on-going and future mapping studies.

This investigation of threshold cutoff values across images and vegetation communities proved informative for this study and will be tested further with nationwide imagery. Because these images were rather small in spatial extent (70 m × 70 m), it was relatively easy to assess the suitability of a threshold value by roaming over the entire image of the plot. For an image with a larger extent this task would be more difficult. Therefore, we believe that the broad guidelines for threshold cutoff values for certain vegetation communities (Figure 4) could be applied to larger images. The high radiometric resolution of digital aerial imagery makes such guidelines useful, because there is greater difficulty in determining a threshold value with 12- or 16-bit digital imagery than with 8-bit film-based digital aerial photography.

It has been demonstrated that this OBIA technique represents a viable approach for quantifying vegetation cover in different vegetation communities in the Northern Chihuahuan desert. While the level of detail is less than that of ground-based measurements, an image analysis approach results in complete classification of the plot, providing baseline information for subsequent studies of land cover change. Due to the transferability of the process tree to additional images or sites, the image analysis approach is more efficient than ground-based measures, especially at the structure group level. While initial algorithm development requires time, subsequent applications of the process tree are relatively fast.

In a previous study, we determined that the breakeven point in time allocated to obtaining ground-based versus image-based measures was eight plots (Laliberte *et al.*, in press). Proximity of plots and time spent on orthorectification of imagery was similar in this study, therefore the time estimates are comparable. The cost of imagery should not be included in a comparison, because imagery is being acquired already for NRI applications.

The ability to classify multiple images efficiently offers the potential to increase the precision of national level inventories by increasing sample locations and to reduce costs by requiring fewer personnel to obtain ground measurements. We are currently implementing the same OBIA approach for a nationwide study in an even broader range of vegetation communities in grazing lands, and are developing additional tools and techniques for potential integration of these techniques into the NIR CEAP Grazing Lands.

### Acknowledgements

This research was funded by the USDA Natural Resources Conservation Service in support of the Conservation Effects Assessment Project, and by the USDA Agricultural Research Service and the National Science Foundation Long-Term Ecological Research Program, Jornada Basin V: Landscape Linkages in Arid and Semiarid Ecosystems. The authors would like to thank Debra Peters and John Anderson for access to the LTER NPP sites, and Hector Godinez-Alvarez, Michelle Mattocks, David Toledo and Justin Van Zee for providing assistance with field data collection. Additional thanks go to the three anonymous reviewers.

### References

- Baatz, M., & Schape, A. (2000) Multiresolution segmentation: an optimization approach for high quality multi-scale image segmentation. In: Strobl, J. & Blaschke, T., eds. *Angewandte Geographische Informationsverarbeitung*, vol. XII, Heidelberg, Wichmann, pp. 12–3.

- Benz, U.C., Hoffmann, P., Willhauck, G., Lingenfelder, I. & Heynen, M. (2004) Multi-resolution, object-oriented fuzzy analysis of remote sensing data for GIS-ready information. *ISPRS Journal of Photogrammetry and Remote Sensing*, vol. 58, pp. 239–258.
- Booth, D.T., & Cox, S.E. (2008) Image-based monitoring to measure ecological change in rangeland. *Frontiers in Ecology and Environment*, vol. 6, no. 4, pp. 185–190.
- Coulter, L.L., & Stow, D.A. (2008) Assessment of the spatial co-registration of multi-temporal imagery from large format digital cameras in the context of detailed change detection. *Sensors*, vol. 8, pp. 2161–2173.
- Definiens (2007) *Definiens Developer 7.0 User Guide*. Definiens AG, Munich.
- Durancik, L.F., Bucks, D., Dobrowolski, J.P., Drewes, T., Eckles, S.D., Jolley, L., Kellogg, R.L., Lund, D., Makuch, J.R., O'Neill, M.P., Rewa, C.A., Walbridge, M.R., Parry, R., & Wetz, M.A. (2008) The first five years of the Conservation Effects Assessment Project. *Journal of Soil and Water Conservation*, vol. 63, no. 6, pp. 185–197.
- Gibbens, R.P., McNeely, R.P., Havstad, K.M., Beck R.F., & Nolen, B. (2005) Vegetation changes in the Jornada Basin from 1858 to 1998. *Journal of Arid Environments*, vol. 61, pp. 651–668.
- Godinez-Alvarez, H., Herrick, J.E., Mattocks, M., Toledo, D., & Van Zee, J. (2009) Comparison of three vegetation monitoring methods: their relative utility for ecological assessment and monitoring. *Ecological Indicators*, vol. 9, pp. 1001–1008.
- Green, K., & Lopez, C. (2007) Using object-oriented classification of ADS40 to map benthic habitats of the state of Texas. *Photogrammetric Engineering and Remote Sensing*, vol. 73, pp. 861–865.
- Herrick, J.E., Van Zee, J.W., Havstad, K.M., Burkett, L.M. & Whitford, W.G. (2005) *Monitoring Manual for Grassland, Shrubland and Savanna Ecosystems. Volume I: Quick Start, and Volume II: Design, Supplementary Methods and Interpretation*, Las Cruces, NM, USDA-ARS Jornada Experimental Range.
- Hinz, A., Doerstel, C., & Heier, H. (2000) Digital modular camera: system concepts and data processing workflow. *International Archives of Photogrammetry and Remote Sensing*, vol. 33, no. B2.
- Hodgson, M.E., Jensen, J.R., Tullis, J.A., Roridan, K.D., & Archer, C.M. (2003) Synergistic use of lidar and color aerial photography for mapping urban parcel imperviousness. *Photogrammetric Engineering and Remote Sensing*, vol. 69, no. 9, pp. 973–980.
- Honkavaara, E., & Markelin, L. (2008) Radiometric performance of digital image data collection - a comparison of ADS40/DMC/UltraCam and EmergeDSS. In: Fritsch, D., ed. *Proceedings of the 51st Photogrammetric Week 2007*, Sept. 2007, Stuttgart, Institut fuer Photogrammetrie, Universitaet Stuttgart, Germany.
- Laliberte, A.S., & Rango, A. (2009) Texture and scale in object-based analysis of sub-decimeter resolution unmanned aerial vehicle (UAV) imagery. *IEEE Transactions of Geoscience and Remote Sensing*, vol. 47, no. 3, pp. 761–770.
- Laliberte, A.S., Rango, A., Havstad, K.M., Paris, J.F., Beck, R.F., McNeely R., & Gonzalez, A.L. (2004) Object-oriented image analysis for mapping shrub encroachment from 1937-2003 in southern New Mexico. *Remote Sensing of Environment*, vol. 93, pp. 198–210.
- Laliberte, A.S., Fredrickson, E.L., & Rango, A. (2007) Combining decision trees with hierarchical object-oriented image analysis for mapping arid rangelands. *Photogrammetric Engineering and Remote Sensing*, vol. 73, no. 2, pp. 197–207.
- Laliberte, A.S., Herrick, J.E., Rango, A., & Winters, C. Acquisition, orthorectification, and object-based classification of unmanned aerial vehicle (UAV) imagery for rangeland monitoring. *Photogrammetric Engineering and Remote Sensing*, vol. 76, no. 6, pp. 661–672.
- Ludwig, J.A., Bastin, G.N., Chewings, V.H., Eager, R.W., & Liedloff, A.C. (2007) Leakiness: a new index for monitoring the health of arid and semiarid landscapes using remotely sensed vegetation cover and elevation data. *Ecological Indicators*, vol. 7, no. 2, pp. 442–454.
- Neumann, K.J. (2008) Trends for digital aerial mapping cameras. *International Archives of the Photogrammetry, Remote Sensing and Spatial Information Sciences*, vol. XXXVII Part B1, pp. 551–554.
- Nusser, S.M., & Goebel, J.J. (1997) The National Resources Inventory: a long term multi resource monitoring programme. *Environmental and Ecological Statistics*, vol. 4, pp. 181–204.

- Pellant, M., Shaver, P., Pyke, D., & Herrick, J.E. (2005) *Interpreting Indicators of Rangeland Health*, version 4, Interagency Technical Reference, Bureau of Land Management, Denver, CO.
- Platt, R.V., & Rapoza, L. (2008) An evaluation of an object-oriented paradigm for land use/land cover classification. *Professional Geographer*, vol. 60, pp. 87–100.
- Rosso, P.H., Klonus, S., Ehlers, M., & Tschach, E. (2008) Comparative properties of four airborne sensors and their applicability to land surface interpretation. *International Archives of Photogrammetry, Remote Sensing and Spatial Information Sciences*, vol. XXXVII, Part B1, pp. 545–550.
- Rouse, J.W., Haas, R.H., Schell, J.A., & Deering, D.W. (1974) Monitoring vegetation systems in the Great Plains with ERTS. In: Freden, S.C., Mercanti, E.P., & Becker, M.A., eds. *Third Earth Resource Technology Satellite (ERTS) Symposium*, NASA, Washington DC, pp. 309–317.
- Sankey, T.T., Moffet, C., & Weber, K. (2008) Postfire recovery of sagebrush communities: assessment using SPOT-5 and very large-scale aerial imagery. *Rangeland Ecology and Management*, vol. 61, pp. 598–604.
- Stow, D., Hamada, Y., Coulter, L., & Zlatina, A. (2008) Monitoring shrubland habitat changes through object-based change identification with airborne multispectral imagery. *Remote Sensing of Environment*, vol. 112, pp. 1051–1061.
- Wainwright, J. (2006) Climate and Climatological Variations in the Jornada Basin. In: Havstad, K.M., Huennecke, L.F., & Schlesinger, W.H., eds. *Structure and Function of a Chihuahuan Desert Ecosystem. The Jornada Basin Long-Term Ecological Research Site*, Oxford, Oxford University Press, pp. 44–80.
- Weber, K.T. (2006) Challenges of integrating geospatial technologies into rangeland research and management. *Rangeland Ecology and Management*, vol. 59, pp. 38–43.
- Yu, Q., Gong, P., Clinton, N., Biging, G., Kelly, M., & Schirokauer, D. (2006) Object-based detailed vegetation classification with airborne high spatial resolution remote sensing imagery. *Photogrammetric Engineering and Remote Sensing*, vol. 72, no. 7, pp. 799–811.